Polarization properties of the retinal nerve fiber layer

HUANG X.-R.[1]

ABSTRACT

Recently developed optical techniques provide quantitative structural measurements of the retinal nerve fiber layer (RNFL). A complete interpretation of these measurements requires understanding of the optical properties of the RNFL. This paper gives a review of the polarization properties and relevant anatomy of the ocular tissues, followed by a thorough discussion of the optical properties of the RNFL. The RNFL reflectance arises from light scattering from cylinders. Microtubules are a major component contributing to the reflectance. The RNFL reflectance exhibits weak intrinsic diattenuation and well preserves polarization. RNFL birefringence varies across the retina; the variation suggests that birefringence depends on the ultrastructure of the nerve fiber bundles, which offers hope that measurement of RNFL birefringence may be able to provide early detection of subcellular changes in glaucoma.

KEYWORDS

Retinal nerve fiber layer, light scattering, cylindrical structures, polarization properties, diattenuation, birefringence

RÉSUMÉ

Des techniques optiques récemment développées permettent d'effectuer des mesures structurelles quantitatives de la couche de fibres nerveuses rétiniennes (CFNR). Une interprétation complète de ces mesures requiert la compréhension des propriétés optiques de la CFNR. Cet article fait état des propriétés de polarisation et de l'anatomie inhérente aux tissus oculaires, et contient une description approfondie des propriétés optiques de la CFNR. La réflectance de la CFNR émane de la diffusion de la lumière depuis les cylindres. Les microtubules sont un composant majeur contribuant à la réflectance. La biréfringence de la CFNR varie au sein de la rétine ; cette variation indique que la biréfringence dépend de l'ultrastructure des faisceaux de fibres nerveuses, ce qui permet d'espérer que la mesure de la biréfringence de la CFNR permettra une détection précoce des changements subcellulaires dans le glaucome.

MOTS-CLÉS

Couche de fibres nerveuses rétiniennes, diffusion de la lumière, structures cylindriques, propriétés de polarisation, diatténuation, biréfringence

.....

[1] *Bascom Palmer Eye Institute, University of Miami School of Medicine, Miami FL*

INTRODUCTION

The retinal nerve fiber layer (RNFL) consists of the unmyelinated axons of retinal ganglion cells gathered into bundles lying just under the retinal surface.[62] The RNFL is damaged in glaucoma and other optic nerve diseases. Clinical observation and red-free fundus photography provide qualitative assessment of the RNFL [35,64] and recently developed optical techniques provide quantitative structural measurements.[26,36,44,66,77,83] Because structural damage often precedes detectable field loss,[1,63-64,70] measurement of the RNFL has achieved an important role in the diagnosis and management of glaucoma. Understanding the optical properties of the RNFL is essential for a complete interpretation of the measurements.

Among the optical properties of the RNFL, its polarization properties are of particular interest because polarized light interacts with matter at the scale of the wavelength of light, meaning that measurement of RNFL polarization properties may reveal information about its microscopic structure.

In optical measurements of the RNFL, the eye acts as an ''optical device'' for passing light to and from the retina. The detected signals are related not only to the properties of the RNFL, but also to the optical properties of other ocular tissues. Because polarized light and polarization sensitive detectors are common in RNFL assessment instruments, polarization properties of the ocular media can act as a confounding variable. Thus, knowledge of the optical properties of other ocular tissues is also necessary for understanding the measured signals.

This paper will give a basic description of polarization, followed by a review of the polarization properties and relevant anatomy of the ocular tissues and a thorough discussion of the reflectance and polarization properties of the RNFL.

POLARIZED LIGHT AND POLARIZATION PROPERTIES OF MATERIALS

Polarization of light describes the behavior of the electric field **E** of a light wave, which changes periodically in time and spatial position (Fig. 1 A, B).[7,45,67] In general the motion of **E** traces an ellipse that represents the polarization state of the light and the light is called elliptically polarized (Fig. 1 C). There are two special cases: circularly and linearly polarized light. When the direction of oscillation of **E** changes randomly in time, the light is depolarized and is called unpolarized light.

When light interacts with an object its polarization changes in a manner determined by the polarization properties of the object.[2,19] Diattenuation is the dependence of the intensity of the exiting beam on the polarization state of the incident beam (Fig. 2 A). Diattenuation can be induced by reflection or absorption; if the change of intensity is due to absorption, diattenuation is also called dichroism. A material has birefringence, when light polarized in a direction with higher refractive index (slow axis) travels more slowly through the material than light polarized in the perpendicular direction with lower refractive index (fast axis) (Fig. 2 B). The delay experienced by the slower component is called retardation (Fig. 2 B). Optical rotation or rotary birefringence causes rotation of polarized light (Fig. 2 C). Depolarization characterizes the transformation of polarized light to unpolarized light (Fig. 2 D). Depolarization in a tissue is closely related to multiple scattering e.g. in a cataractous lens. Polarizance is the transformation of unpolarized light to polarized light (Fig. 2 E), as occurs for example, when light is reflected from an oblique, smooth surface. Thus, polarized sun glasses remove windshield reflections even though the incident sunlight is unpolarized.

In biological media, very often polarization properties indicate structural arrangements.[2] For example, birefringence in tissues is frequently due to the presence of asymmetrical oriented structures of a given refractive index (such as, collagen fibrils, microtubules, actin, and myosin filaments) dispersed in a medium of different refractive index (such as, cytoplasm, extracellular flu-

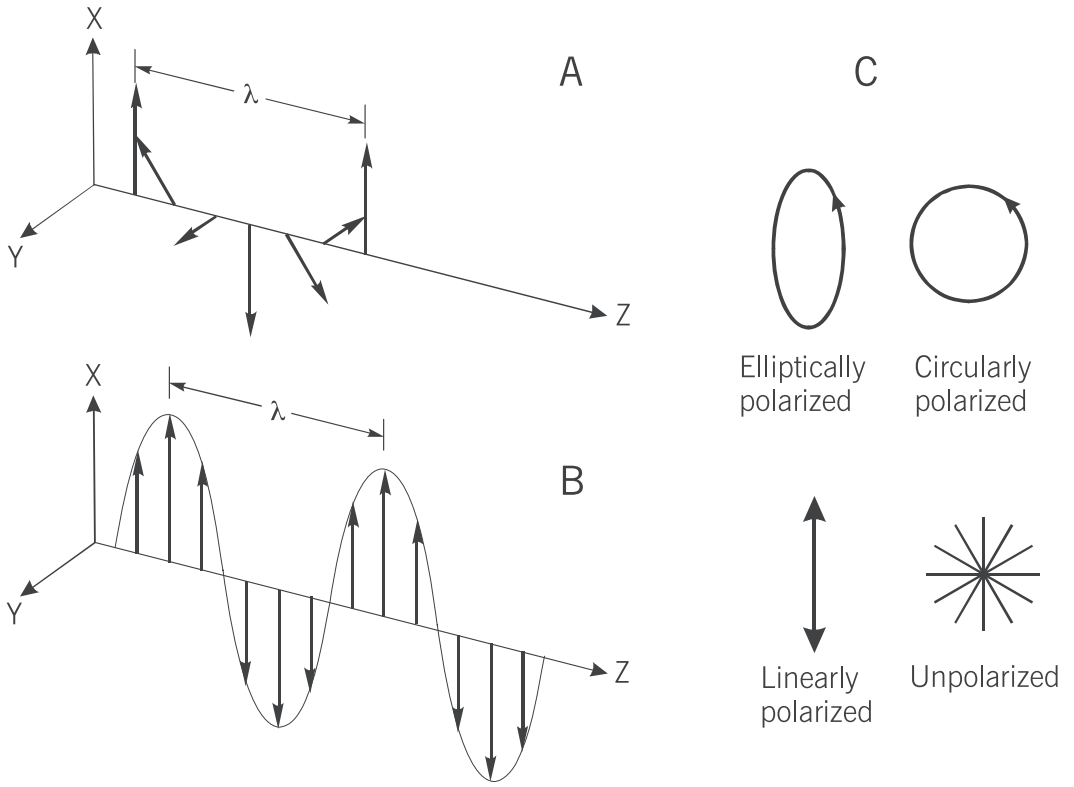

Fig. 1. Polarization of light. A) A light wave, propagating along the Z axis, is described as an oscillating electric vector **E** (arrows). The motion of **E** in general traces an ellipse when the tip of **E** is projected onto a plane perpendicular to the propagation direction; B) the light is linearly polarized when E oscillates in a plane; C) representation of the polarization states of light. λ: wavelength.

id). This type of birefringence, known as form birefringence, is directly related to an ordered arrangement of structures, whose size is large compared with the dimensions of molecules but small compared with the wavelength of light (Fig. 3).[2,7] In a birefringent material, there is at least one direction along which an incident light has equal propagation velocities regardless of its polarization state. Such a direction is called an optic axis (Fig. 3).[2,45,67] Note that in the examples shown in figure 3 light propagating perpendicular to the optic axis experiences maximum retardation.

OPTICAL ANATOMY AND POLARIZATION PROPERTIES OF OCULAR TISSUES

The optical function of the eye is to form the image of an object onto the retina. As illustrated in figure 4, light is refracted by the cornea and the lens, then traverses the vitreous humor, and finally forms a sharp image on the retina. Meanwhile light is absorbed, reflected and scattered by the fundus.[9,23,74]

The healthy cornea is a clear, transparent tissue that forms the strongest refracting surface of the eye. The cornea is mainly made up by the stroma (nine-tenths of the corneal thickness), which consists of about 200 sheets of collagenous fibers, the stromal lamellae, lying parallel to the surface.[9,58] The fibers within each individual lamella are parallel, but the fibers in adjacent lamellae make large angles with one another. The stack formed by the stromal lamellae displays form

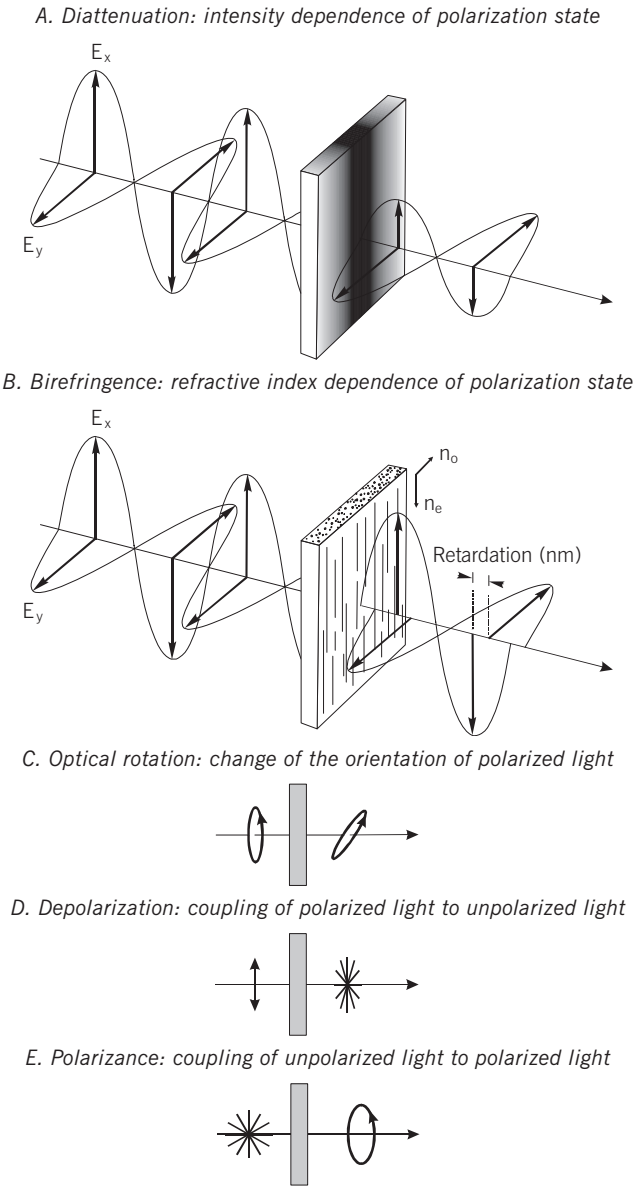

Fig. 2. Polarization properties. E_x, E_y: components of the electric vector E; n_o, n_e: refractive indexes.

birefringence with the fast axis perpendicular to the corneal surface.[8-9] Meanwhile, due to preferred direction of the fibers, rather than random orientation, the cornea becomes biaxial with the slowest axis parallel to the surface.[9,72] For a light beam approximately perpendicular to the corneal surface, the cornea behaves as a linear retarder with the slow axis parallel to the surface. In an individual eye, the retardation is approximately constant in the central cornea but slightly increases with eccentricity.[13,55,72] Among subjects the retardation and axis in the central cornea varies over a wide range (Fig. 5).[31,55,79] The maximum values of corneal retardance can be large enough to affect the polarization state of a measuring beam and should be regarded as a significant confounding variable for any polarization sensitive technology.

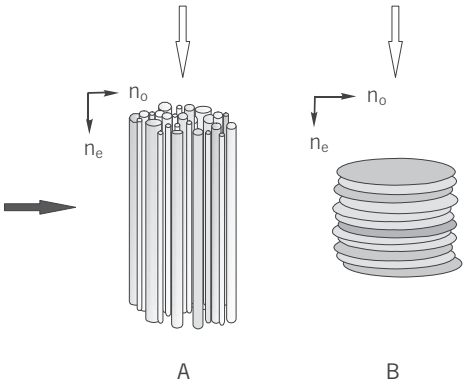

Fig. 3. Form birefringence. A) due to parallel fibrils; B) due to parallel discs. Black arrow: the propagation direction with maximum birefringence; white arrows: optic axis along which no retardation is introduced to an incident light; n_o, n_e: refractive indexes.

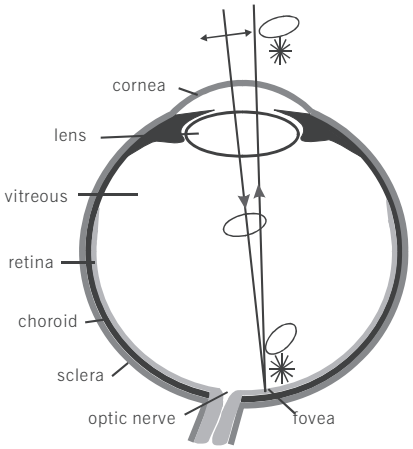

Fig. 4. Light beam path in the eye. The polarization state of the beam changes along the path due to the polarization properties of the ocular tissues (see text).

The biconvex lens can be divided into two regions: the nucleus, the central region of the lens, and the cortex, the outer layers, which has an ''onion-like'' or layered structure.[18] The lens also presents birefringence, but has small retardation in comparison to the cornea (by a factor of 10).[4,8-9,11,14,76] The weak birefringence probably is due to the cancellation of the intrinsic (resulting from an asymmetrical alignment of chemical bonds, ions or molecules) and form birefringence of the lenticular fibers.[4,11]

Due to Fresnel reflection at boundaries between differing media, diattenuation is expected for light interacting with the cornea and lens, except for normal incidence.[18,20] Multiple scattering occurring in the cornea and lens results in depolarization.[28,57] However, both the diattenuation and depolarization have been found very weak in the healthy cornea and lens.[13] On the other hand, depolarization increases in older and cataractous lenses and can significantly reduce the detected signals that use the reflected light from the fundus.[13-14,34] The transparent and gel-like vitreous is 99 percent water and has no known polarization properties.

The posterior portion of the eye contains multiple layers that absorb, reflect, and scatter light.[23,27,49,80] The inner limiting membrane (ILM) separates the retina from the vitreous and, being a smooth surface that provides a refractive index transition, produces specular reflection.[23,30,46] The RNFL lies just under the retinal surface and its optical properties and relevant

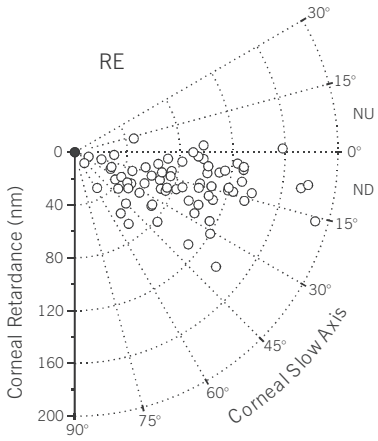

Fig. 5. The central corneal birefringence of 73 subjects plotted in polar coordinates: a line connecting a point and the origin has the same orientation as the corneal slow axis and a length equal to the corneal retardance. Retardance values are for a double-pass through the cornea. Approximately 80 % of retardance values are uniformly distributed between 40 and 140 nm; the mode of the slow axis distribution lies between 10° and 20° nasally down. RE: right eye; NU: nasally up; and ND: nasally down. Adapted from Knighton[55] with permission.

anatomy will be discussed in detail later. Beneath the RNFL are the ganglion cell layer, inner plexiform layer, inner nuclear layer, outer plexiform layer, outer nuclear layer, and outer limiting membrane, which together act as a weakly scattering matrix with some laminar structure.[29,43] The photoreceptor layer is composed of the rods and cones, which can be divided into two optical regions, the inner segment layer (ISL) and outer segment layer (OSL). Light can experience strong absorption in the OSL due to the photolabile visual pigments but clinical examination uses sufficient light to bleach the visual pigments so that they do not alter fundus reflectance.[10] For optical techniques using infrared light, the absorption of the visual pigments is so weak that the OSL is nearly transparent. Because the outer segments contain densely packed membranous discs, the OSL exhibits diattenuation and birefringence.[68] However, the discs are arranged perpendicular to the long thin cell bodies of the photoreceptors, the optical axes are along the cell bodies and the OSL has negligible effect on the polarization properties of the normally incident light (Fig. 3 B).

The retina is apposed to the pigment epithelium (RPE), a single layer of epithelial cells with processes that surround the outer segments.[33] The RPE captures stray light to prevent back reflection, especially at short and medium wavelengths, due to light absorption by granules of the dark-brown pigment melanin.[23,74] Additionally, the melanin granules contribute to scattering in the infrared. Light is, therefore, significantly attenuated in the RPE. The choroid, separated from the RPE by Bruch's membrane, contains blood vessels and pigmented melanocytes. Light suffers absorption and multiple scattering because of the hemoglobin and melanocytes.[23,71,74] The outermost layer of the eye is the sclera, the thick white coat of the eye that is often regarded as a diffuse reflector.[23,74]

The retina has a capillary network lying in the outer retina with density varying with the thickness of the RNFL. Except for large vessels, the retinal circulation has little influence on the fundus reflectance.

The optic disc, where the optic nerve fibers leave the retina to the brain, and the fovea, the region of highest visual acuity, are specialized areas in the human eye. The tissues of the optic disc are highly scattering.[23] The fovea and its surrounding region, the macula, are recognized in histology by the presence of the oblique and elongated Henle's fibers (photoreceptor axons). The macula contains yellow pigment that strongly absorbs blue light.[27] The phenomenon of "Haidinger's Brushes" (faint blue and yellow brushes seen if a white surface is viewed through a rotat-

ing polarizer) has been explained by the dichroism of the macular pigment or the form birefringence of Henle's fibers.[6,12] The birefringence of the macula behaves as a linear retarder with radially distributed slow axes and approximately constant retardation.[12,83] This property has been used to measure the corneal birefringence in vivo.[83]
Although the polarization properties of the ocular tissues do not affect image formation on the retina, they must be taken into account if polarized light is used in fundus examination or measurement. In summary, the ocular tissues with the most effect on the polarization state of the incoming light include the cornea, the lens, Henle's fibers at the macula and the RNFL around the optic nerve head (ONH). The picture of a linearly polarized light passing through the eye is that the light becomes elliptically polarized when passing through the cornea and lens due to their birefringence; additional retardation is added and partial depolarization occurs at the fundus because of the birefringence of Henle's fibers or the RNFL, and the scattering processes at the fundus; the polarized part is affected again on its return path (Fig. 4).

OPTICAL PROPERTIES OF THE RNFL

Knowledge of the optical properties of the RNFL may help one to understand qualitatively the brightness of the clinically observed RNFL and can be valuable to improve quantitative measurements of the RNFL. This section summarizes current understanding of the RNFL reflectance properties and their mechanisms and discusses implications for clinical observation and assessment of the RNFL.

Relevant anatomy of the RNFL

The human RNFL is formed by the unmyelinated axons of retinal ganglion cells, and appears nearly transparent. The axons, membrane-enclosed processes with diameters of 0.1-4 μm, are gathered into bundles.[33,59-60,62] Axons themselves form parallel arrays containing cylindrical organelles: microtubules (MTs), neurofilaments, and mitochondria (Fig. 6). Axonal membranes form cylindrical shells enclosing the axonal cytoplasm and have the typical structure of cell membranes, 6-10 nm thick phospholipid bilayers with embedded proteins. A lipid bilayer exhibits intrinsic birefringence due to hydrocarbon molecular chains that lie perpendicular to its surface,[68] but this birefringence is weak so that the axonal membrane can be treated as an optically isotropic substance in most circumstances. Microtubules are tubular organelles with an outer diameter about 25 nm, an inner diameter about 15 nm, and a length of 10-25 μm. Microtubules are dynamic structures formed by the polymerization of the dimeric protein tubulin that can be disrupted by anti-mitotic drugs (e.g. colchicine).[21] Microtubules also exhibit weak intrinsic birefringence with the slow axis parallel to the microtubule.[61,65] Neurofilaments are stable protein polymers with a diameter of about 10 nm. Mitochondria are ellipsoidal organelles with approximately 10:1 length to thickness ratio and diameters of 0.1-0.5 μm. In summary, anatomically the RNFL possesses four cylindrical substructures: the cell membranes of axons; microtubules and neurofilaments as thin fibrils (diameters much less than the wavelength of light); and mitochondria.[81] Mammalian RNFL, including human, in addition to axons, also contains the processes of glial and Muller cells running parallel to the axons.[59]
The thickness of the RNFL is strongly location-dependent.[60,75] In human, the RNFL thickness varies from 10 μm to 400 μm. The thickness decreases with increasing distance from the ONH. Around the ONH, the RNFL is thicker in superior and inferior regions and thinner in temporal and nasal regions.

The RNFL reflectance is highly directional

The microscopic appearance of the RNFL leads to the assumption that the RNFL reflectance arises from light scattered by cylindrical structures. Investigations by Knighton et al. show that

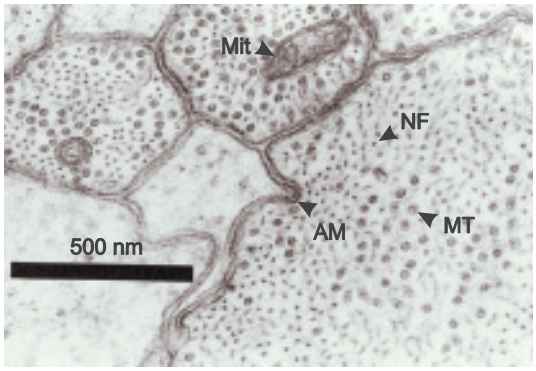

Fig. 6. Cross section of the rat RNFL reveals the axonal membranes (AM), microtubules (MT), neurofilaments (NF), and mitochondria (Mit)

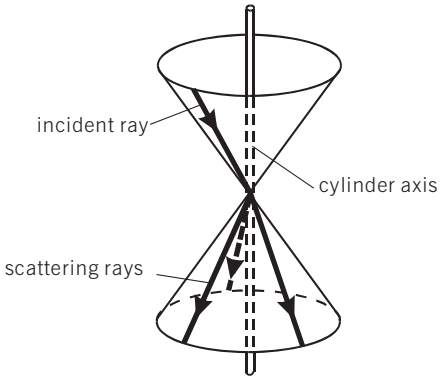

Fig. 7. The geometry of cylinder scattering. The light scattered by a cylinder is confined to a conical sheet coaxial with the cylinder axis. The apex angle of the cone is the twice the angle between the cylinder axis and the incident ray.

the reflectance of the RNFL is very directional and exhibits the same geometry as light scattering by a cylinder (Fig. 7).[5,48,52,54,73] Retinal nerve fiber bundles observed near the predicted scattered cone appear as bright striations against a dark background (Fig. 8 A).[48,52] However, the reflectance falls very rapidly from the peak, as seen in figure 8 B; at 30° away from the peak reflectance the bundles are entirely invisible.

Due to the misalignment of cylinders and finite apertures of light source and camera, the measured scattered sheet is broadened, as shown in figure 8 C. The angular spread functions, fitted to the measured data, fall into two groups by wavelength; the width for the longer wavelengths (660 nm, 830 nm) was significantly larger than for the shorter wavelengths (420 nm, 500 nm).[52] This suggests that across wavelength the RNFL reflectance involves different mechanisms.

The directionality of the RNFL reflectance is an important variation source in clinical observation and optical measurements, because the intensity of a nerve fiber bundle depends on the relative positions of the incident and exiting beams and bundle location on the fundus.[54] An example of the directionality phenomenon is seen in optical coherence tomography (OCT) images of the optic disc, in which the RNFL reflectance disappears as the bundles turn to enter the disc.[49]

The RNFL reflectance is proportional to its thickness

As commonly assumed by clinicians, the RNFL reflectance is proportional to its thickness.[50] The relation between reflectance and the thickness is confounded, however, by the directional

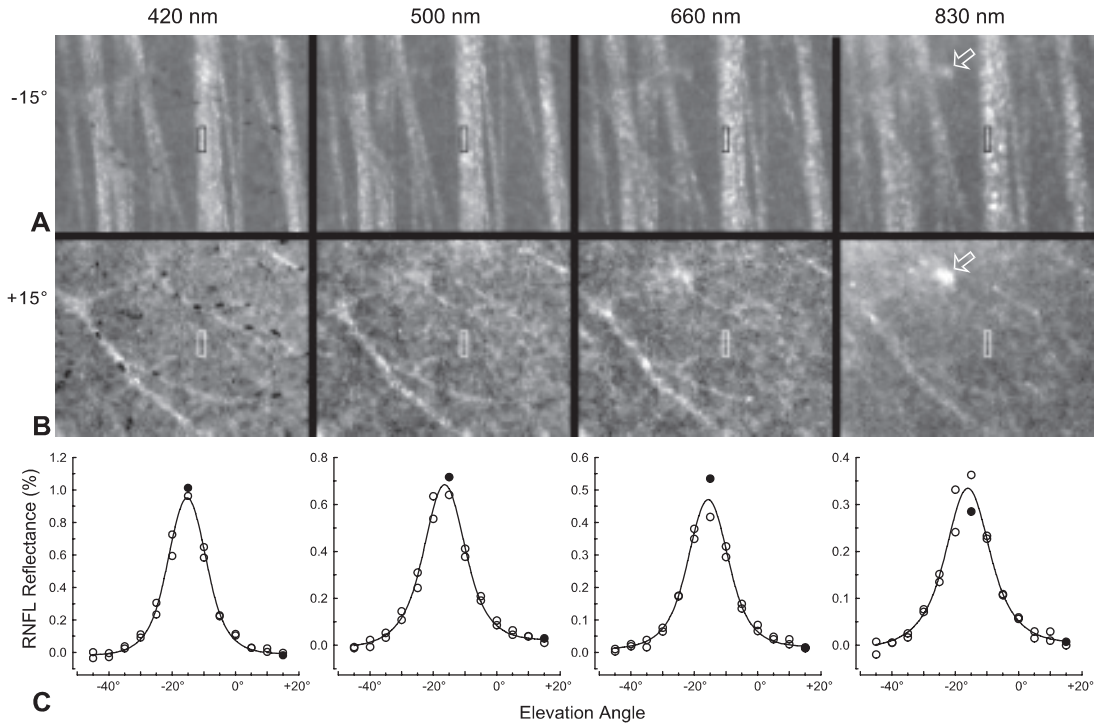

Fig. 8. The directional reflectance of the rat RNFL at four wavelengths. The RNFL reflectance was measured at the small area indicated. A) Images obtained with the light source near the predicted cone (elevation = (15°); B) images obtained with the light source 30° above the predicted cone (elevation = +15°); C) angular spread of the scattered light measured in two vertical scans (circles). The filled circles correspond to the images in (A) and (B). The solid line fitted to the measured data is a symmetrical decaying exponential convolved with the instrument aperture function. Image size: 320 μm $\times$ 250 μm. Reproduced with permission from Knighton.[52]

reflectance of the RNFL. For a localized RNFL defect, where affected bundles lie adjacent and parallel to less affected bundles, the observed brightness variation corresponds to a variation in thickness. Equally thick areas located in different regions of the fundus are not necessarily equally bright, however, and the brightness of a given area will depend on the geometry of observation, as mentioned earlier.

A corollary of the proportionality is that the reflected light arises from throughout the entire volume of the RNFL, which is demonstrated directly by OCT. Volume reflectance may affect those techniques that use the reflected light to establish the topography of the RNFL surface, such as confocal scanning laser tomography. The accuracy of locating the surface is determined by the uncertainty in the location of origin of the reflected light as well as the geometry of observation.

The RNFL reflectance is wavelength dependent

The reflectance of the RNFL varies with wavelength (λ);[47,52] reflectance declines rapidly with increasing wavelength at shorter wavelengths (< 560 nm), declines slowly between 560 nm to 700 nm, and declines rapidly again after 700 nm (Fig. 9). The shape of a reflectance spectrum depends on incident and scattering angles (Fig. 9 B). As discussed later, spectral measurements provide data for modeling the mechanisms of the RNFL reflectance.

Microtubules contribute to the RNFL reflectance

The steep slope of the RNFL reflectance spectrum at short wavelengths suggests that thin cylinders contribute to the scattering. MTs and neurofilaments within axons are two likely candi-

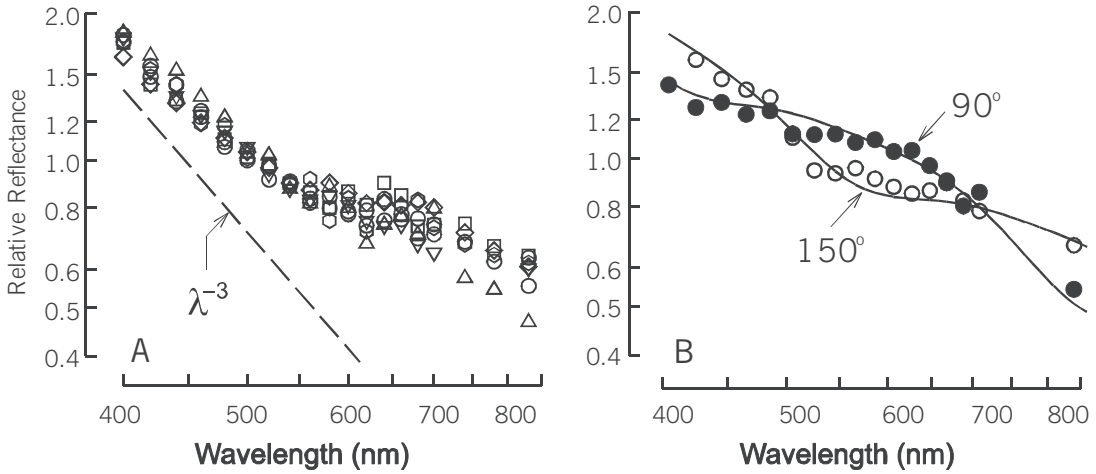

Fig. 9. The RNFL relative reflectance spectra. A) The reflectance spectra of seven rat RNFL normalized to the mean. The scattering angles were about 180° or 170°. The dashed line shows λ^{-3} spectral dependence for a random array of parallel thin cylinders; B) spectral reflectance of the rat RNFL at two scattering angles of 150° and 90° in one experiment. The smooth curves show the fit of a two-mechanism cylindrical scattering model (see text) Adapted from Knighton [52] with permission.

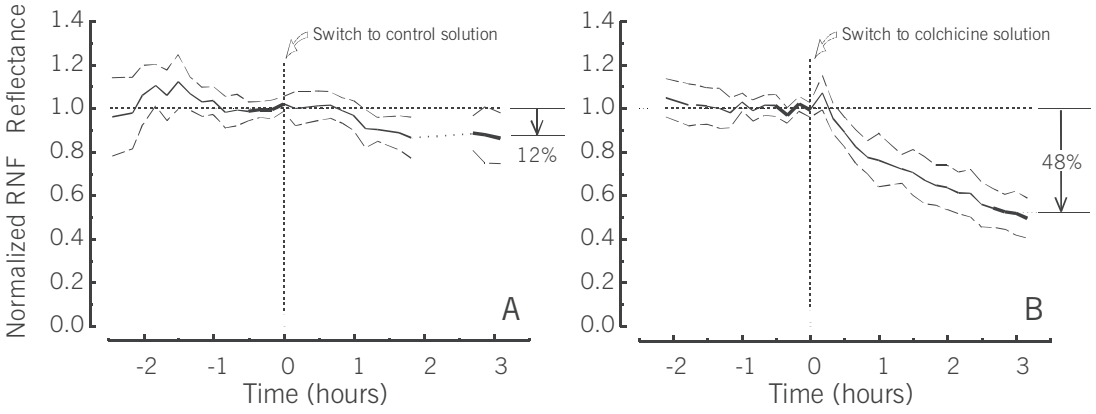

Fig. 10. A) A control experiment demonstrated the stability of the RNFL reflectance; B) colchicine caused the RNFL reflectance to decline. Solid lines are the mean of the normalized and averaged RNFL reflectance with one standard deviation above and below the means (dashed lines). Adapted from Knighton [51] with permission.

dates. The role of MTs in the RNFL reflectance was examined by using the anti-mitotic agent colchicine to prevent polymerization of MTs.[51] In the experiment illustrated in figure 10, the peak reflectance of toad RNFL was measured at 440 nm over an extended period. During a 2 hour baseline, the preparation was perfused with a solution containing no colchicine. During a 3 hour treatment period, the solution was switched either to a solution containing colchicine or to a control solution identical to the baseline solution. The control experiments demonstrate that the RNFL reflectance is stable (Fig. 10 A). In contrast, the RNFL reflectance declined dramatically during colchicine treatment (Fig. 10 B). These results indicate that, at least at short wavelengths, light scattered by MTs is a major component of the RNFL reflectance.

Evidence for two scattering mechanisms

The dependence of angular spread functions on wavelength (Fig. 8 C) suggests that multiple mechanisms underly the RNFL reflectance. Although MTs contribute to the RNFL reflectance,[51]

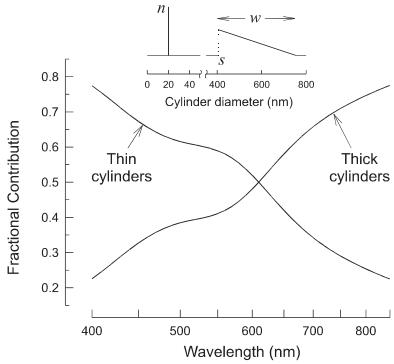

Fig. 11. Fractional contributions of hypothetical thin and thick cylinders to the measured spectra shown in figure 9B. The two-mechanism cylindrical scattering model has three free parameters. The inset shows the ''triangle'' distribution of the thick cylinder diameters. For a unit area under this distribution there are *n* thin cylinders. Adapted from Knighton [52] with permission.

the measured RNFL spectra differ from the spectrum of an array of thin cylinders only (dashed line in figure 9 A), which suggests that thicker cylinders also contribute to the reflectance. A two-mechanism cylindrical scattering model successfully describes the measured spectra (Fig. 9 B).[52] The model suggests that both thin and thick cylinders contribute to the RNFL reflectance with the thin cylinder mechanism dominating the reflectance at short wavelengths and the thick cylinder mechanism dominating at long wavelengths (Fig. 11). Thus, assessments based on the RNFL reflectance at different wavelengths (e.g. photography with red-free light and OCT with near-infrared light) may relate to different structures. The anatomic basis for the thick cylindrical mechanism is unclear.

In summary, optically the RNFL behaves as a uniform thick array of approximately parallel cylinders. The identities of the cylinders and their contributions to the RNFL reflectance, however, are only partially known.

POLARIZATION PROPERTIES OF THE RNFL

Clinical studies suggest that direct detection of changes in the RNFL can provide earlier diagnosis of glaucoma and other neuropathies. Several optical methods have been developed to assess the RNFL quantitatively and provide a promising way for clinical diagnosis and management of these diseases.[26,36,44,66,77,83] In these techniques polarized light and/or polarization sensitive detectors are commonly used. Knowledge of polarization properties of the RNFL is essential for understanding these methods and may help reduce their measurement variability and improve their assessment ability. Besides, polarization properties of the RNFL are directly related to its ultrastructure; measurement of these properties may provide a means to detect early structural change.

The RNFL reflectance has weak intrinsic diattenuation

Diattenuation can be caused by reflection or absorption but, because the RNFL is nearly transparent, dichroism is unlikely.[19-20,53] The RNFL reflectance, however, may exhibit diattenuation due to scattering by the preferential orientation of cylindrical structures.[38,81] Diattenuation also depends strongly on the geometry of the incident and scattering beams.[5,20,73] The diattenuation inherent in a measurement geometry is derived from the Rayleigh-Gans (R-G) theory of light scattering by particles. It forms a limiting value from which intrinsic diattenuation will deviate. In vitro experiments show that RNFL diattenuation is close to the R-G limit (Fig. 12), which

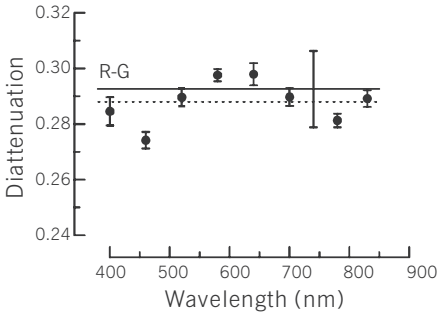

Fig. 12. Diattenuation spectrum of one bundle in a fixed rat retina. Filled circles with error bars: measured diattenuation and estimated measurement error; dashed line: mean diattenuation across the wavelengths; solid line and vertical error bar at 740 nm: R-G limit of this particular measurement geometry and estimated uncertainty.

suggests that the RNFL reflectance has weak intrinsic diattenuation.[39] RNFL diattenuation is also found to be low in human eyes.[26]
Weak diattenuation of the RNFL allows modeling the RNFL as a linear retarder in optical measurements, such as scanning laser polarimetry (SLP) and polarization sensitive OCT.[22,56,82] However, diattenuation dependence of the measurement geometry, i.e. the Rayleigh-Gans mechanism, has to be taken into account in any clinical technology for assessing the RNFL diattenuation.[3]

The RNFL is a polarization preserving reflector

Degree of polarization (DOP), a measure of the polarized portion of a partially polarized beam, is often used to characterize the amount that polarization is preserved when light is reflected by a tissue.[19,26,29,71] Decrease of DOP results from depolarization. Physically, depolarization is closely related to multiple scattering or incoherent scattering processes.[5,73] DOP has been measured in human fundus; a nearly 90 % DOP in the backscattered light from the fovea has been found, and DOP ranging from 50 % to 80 % is measured around the ONH.[26,72] These measurements, however, include light reflected from the retina and its underlying tissues. DOP of the light reflected from the RNFL alone is found to be nearly 100 % for wavelengths ranging from blue to near infrared.[39] The result suggests that the RNFL reflectance comes from single scattering and that the RNFL is a polarization-preserving reflector. High DOP may contribute to the RNFL appearance as a highly scattering layer in OCT.[36]

The RNFL birefringence depends on the structure of nerve fiber bundles

The RNFL exhibits form birefringence due to cylindrical structures in the retinal axons.[24-26,32,37,81] The birefringence of the RNFL can be well demonstrated qualitatively, when a retina is viewed in transmission between two crossed polarizers (Fig. 13).[37] The value of birefringence, Δn, can be calculated as retardance per unit thickness (birefringence is a dimensionless number; however, units of nm/μm explicitly acknowledge the relation between retardance and thickness and, hence, are used in this paper). Δn of the RNFL is approximately constant across visible wavelengths and the near infrared.[37] The result is consistent with a mechanism of form birefringence from thin cylindrical organelles. Newly experiments suggest that microtubules substantially contribute to the RNFL birefringence.[42]
Birefringence is a tissue property. Theoretical models of RNFL birefringence show that Δn is determined by the volume fraction and relative refractive index of relevant cylinders and the refractive index of the surrounding medium.[32,81] Differences in Δn, therefore, must necessarily reflect differences in the density or composition of the axons that make up the RNFL, i.e. Δn depends

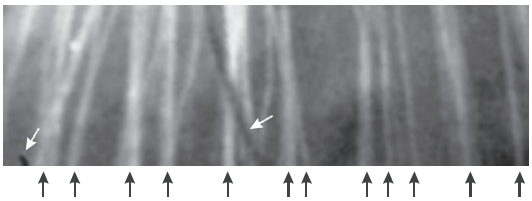

Fig. 13. Rat retina, isolated free from the pigment epithelium, viewed in transmission at 500 nm between two crossed polarizers, which are set at 45° with respect to the nerve fiber bundles. Birefringence causes bundles to appear as bright stripes (black arrows). Blood vessels (white arrows) appear as black due to strong absorption by hemoglobin in red blood cells. Image size: 1152 μm wide × 360 μm high.

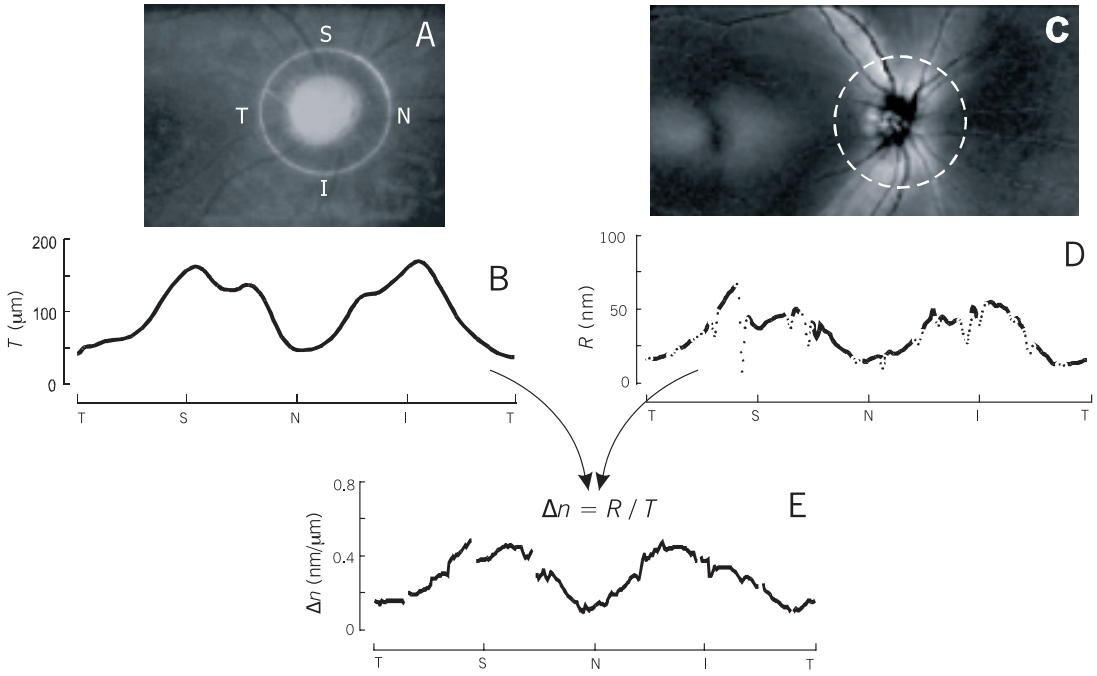

Fig. 14. Birefringence measured by OCT and SLP. A) OCT video fundus image of the peripapillary OCT scan path proceeding from temporal retina through superior, nasal, inferior, and back to temporal retina (TSNIT); B) RNFL thickness profile along the scan path; C) RNFL retardance image obtained by SLP with compensation for anterior segment birefringence. Dashed line circle is the scan path transferred from OCT by image registration; D) profile of the single-pass retardance around the path. Retardances on retina vessels (dots) are excluded from data analysis; E) birefringence profile calculated from the pair of *R* and *T* profiles. Adapted from Huang [41] with permission.

directly on the ultrastructure of the nerve fiber bundles. In diseases such as glaucoma, measurement of Δn may provide a means for the detection of subcellular structure changes prior to ganglion cell death.

RNFL birefringence has been studied by several investigators.[15-17,40-41,78] Recently, the distribution of RNFL birefringence in human has been studied by two different methods: by polarization sensitive OCT and by combining commercially available technologies of OCT and SLP.[17,41] The findings from the two methods are similar. Because it may be more generally available, the second method is described here. The RNFL thickness (T) is measured by OCT on a circular scan path around the ONH (Fig. 14 A, B); the RNFL retardance (*R*) is measured by SLP and the R values along the same scan path are derived from the retardance image (Fig. 14 C, D). A Δn profile (Fig. 14 E) is then calculated from Δn = R/T. A remarkable feature of the calculated

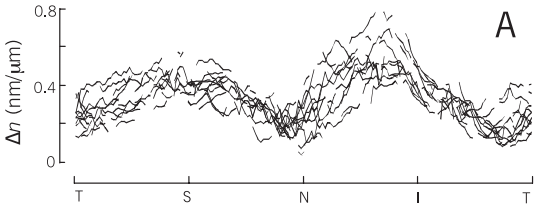

Fig. 15. Most normal subjects show variation in Δn on a path across nerve fiber bundles. Δn profiles on a 3.4 mm diameter circle around the ONH in 12 eyes measured in one study group (A) and 11 eyes in a second study group (B). Adapted from Huang [41] with permission.

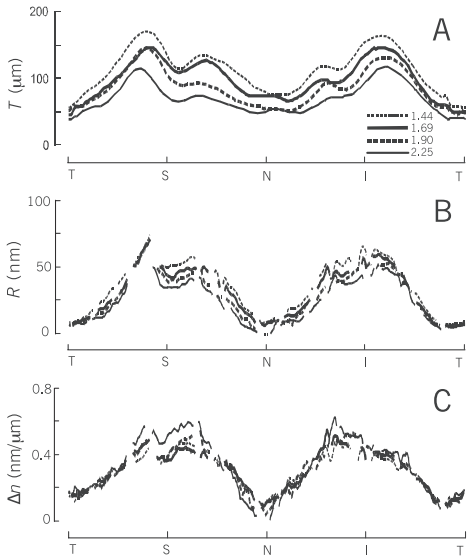

Fig. 16. Similar birefringence variation on paths of different radii. A) *T* profiles obtained on OCT scan circles with radii of 1.44, 1.69, 1.90, and 2.25 mm, as indicated; B) corresponding *R* profiles from a single SLP image; C) calculated Δn profiles. Adapted from Huang [41] with permission.

Δn shown in figure 14 E is that Δn varies significantly along the scan path that crosses the nerve fiber bundles. Similar appearance is found in most of studied subjects as shown in figure 15; Δn varies around the ONH with peaks in superior and inferior RNFL and valleys in temporal and nasal RNFL (Δn ranges from approximately 0.24 to 0.40 nm/μm). Variation of Δn around the ONH is consistent with the fact that the density and composition of axons differ between the retinal areas.[60] In contrast to the variation around the ONH, Δn is not expected to change along bundles because once together axons remain bundled together, Δn measured on multiple scan circles confirms this expectation (Fig. 16). Together, the variation of Δn across nerve fiber bundles with constant Δn along bundles, imply that RNFL birefringence directly depends on the underlying structure of nerve fiber bundles, which offers hope that measurement of RNFL birefringence may be able to detect subcellular changes in glaucoma before irreversible loss of axons. To explore this possibility, future studies must measure RNFL birefringence in patients with various degrees of glaucomatous damage.

CONCLUSION

The RNFL reflectance arises from light scattering from cylinders. The directionality of the RNFL reflectance may be an important source of variability in clinical assessment methods. The RNFL

reflectance exhibits weak intrinsic diattenuation and well preserves polarization. RNFL can be modeled as a retarder in optical measurements. RNFL exhibits form birefringence. RNFL birefringence, as a tissue property, depends on the ultrastructure of nerve fiber bundles. Birefringence measurements may, therefore, provide an early indicator of structural changes caused by glaucoma.

ACKNOWLEDGMENTS

The author sincerely thanks Robert W. Knighton, PhD for invaluable suggestions for and timely reviews of the manuscript.

REFERENCES

(1) AIRAKSINEN P.J., DRANCE S.M., DOUGLAS G.R., MAWSON D.K., NIEMINEN H. – Diffuse and localized nerve fiber loss in glaucoma. Am J Ophthalmol 1984; 98: 566-571
(2) BENNETT H.S. – The microscopical investigation of biological materials with polarized light. In: McClung C.E. (ed.) Handbook of microscopical technique. Hafner Pub Co, New York NY1961
(3) BENOIT A.M., NAOUN K., LOUIS-DORR V., MALA L., RASPILLER A. – Linear dichroism of the retinal nerve fiber layer expressed with Mueller matrices. Appl Opt 2001; 40: 565-569
(4) BETELHEIM F.A. – On the optical anistropy of lens fiber cells. Exp Eye Res 1975; 21: 231-234
(5) BOHREN C.F., HUFFMAN D.R. – Absorption and scattering of light by small particles. John Wiley & Sons, New York NY 1983
(6) BONE RA. – The role of macular pigment in the detection of polarized light. Vision Res 1980; 20: 213-220
(7) BORN M., WOLF E. – Principles of optics: electromagnetic theory of propagation, interference, and diffraction of light. Cambridge University Press, Cambridge 1999; 24-38; 837-840
(8) BOUR L.J., LOPES CARDOZO N.J. – On the birefringence of the living human eye. Vision Res 1981; 21: 1413-1421
(9) BOUR L.J. – Polarized light and the eye. In: Charman W.N. (ed.) Vision and visual dysfunction: visual optics and instrumentation. CRC Press Inc, Boca Raton FL 1991; 310-325
(10) BOWMAKER J.K., DARTNALL H.J.A. – Visual pigments of rods and cones in a human retina. Journal of Physics 1980; 298: 501-511
(11) BRINK H.B., KLEIN – Birefringence of the human crystalline lens in vivo. J Opt Soc Am 1991; 8: 1788-1793
(12) BRINK H.B., VAN BLOKLAND G.J. – Birefringence of the human foveal area assessed in vivo with Mueller-matrix ellipsometry. J Opt Soc Am 1988; 5: 49-57
(13) BUENO J.M., JARONSKI J. – Spatially resolved polarization properties for in vitro corneas. Ophthal Physiol Opt 2001; 21: 384-392
(14) BUENO J.M., CAMPBELL M.C.W. – Polarization properties of the in vitro old human crystalline lens. Ophthal Physiol Opt 2003; 23: 109-118
(15) CENSE B., CHEN T.C., PARK B.H., PIERCE M.C., DE BOER J.F. – In vivo depth-resolved birefringence measurements of the human retinal nerve fiber layer by polarization-sensitive optical coherence tomography. Opt Let 2002; 27: 1610-1612
(16) CENSE B., CHEN T.C., HYLE PARK B., PIERCE M.C., DE BOER J.F. – In vivo birefringence and thickness measurements of the human retinal nerve fiber layer using polarizaion-sensitive optical coherence tomography. J Biomed Opt 2004; 9: 121-125
(17) CENSE B., CHEN T.C., PARK B.H., PIERCE M.C., DE BOER J.F. – Thickness and birefringence of healthy retinal nerve fiber layer tissue measured with polarization sensitive optical coherence tomography. Invest Ophthalmol Vis Sci 2004 (in press)
(18) CHARMAN W.N. – Optics of the human eye. In: Cronly-Dillon J.R. (ed.) Vision and visual dysfunction. CRC Press Inc, Boca Raton FL 1991; 1-26
(19) CHIPMAN R.A. – Polarimetry. In: Bass M., van Stryland E.W., Williams D.R., Wolfe W.L. (eds.) Handbook of optics. McGraw-Hill Inc, New York NY 1995; 22.21-22.37
(20) COLLETT E. – Polarized light: fundamentals and applications. Marcel Dekker Inc, New York NY 1993; 163-185

(21) DARNELL J., LODISH H., BALTIMORE D. – Molecular cell biology. Scientific American Books, New York NY 1990; 820-822
(22) DE BOER J.F., MILNER T.E. – Review of polarization sensitive optical coherence tomography and Stokes vector determination. J Biomed Opt 2002; 7: 359-371
(23) DELORI F.C., PFLIBSEN K.P. – Spectral reflectance of the human ocular fundus. Applied Optics 1989; 28: 106-1077
(24) DREHER A.W., REITER K. – Retinal laser ellipsometry - a new method for measuring the retinal nerve-fiber layer thickness distribution. Clin Vis Sci 1992; 7: 481-488
(25) DREHER A.W., REITER K. – Scanning laser polarimetry of the retinal nerve fiber layer. In: Goldstein D.H., Chipman R.A. (eds.) Proc SPIE 1992; 34-41
(26) DREHER A.W., REITER K., WEINREB R.N. – Spatially resolved birefringence of the retinal nerve-fiber layer assessed with a retinal laser ellipsometer. Appl Opt 1992; 31: 3730-3735
(27) FINE B.S., YANOFF M. – Ocular histology. Harper & Row Publisher Inc, New York NY 1979
(28) FREUND D.E., MCCALLY R.L., FARRELL R.A. – Direct summation of fields for light scattering by fibrils with applications to normal corneas. Appl Opt 1986; 25: 2739-2746
(29) GLOESMANN M., HERMANN B., SCHUBERT C., SATTMANN H., AHNELT P.K., DREXLER W. – Histologic correlation of pig retina radial stratification with ultrahigh-resolution optical coherence tomography. Invest Ophthalmol Vis Sci 2003; 44: 1696-1703
(30) GORRAND J.M., DELORI F.C. – Reflectance and curvature of the inner limiting membrane at the foveola. J Opt Soc Am 1999; 16: 1229-1237
(31) GREENFIELD D.S., KNIGHTON R.W., HUANG X.R. – Effect of corneal polarization axis on assessment of retinal nerve fiber layer thickness by scanning laser polarimetry. Am J Ophthalmol 2000; 129: 715-722
(32) HEMENGER R.P. – Birefringence of a medium of tenuous parallel cylinders. Appl Opt 1989; 28: 4030-4034
(33) HOGAN M.J., ALVARADO J.A., WEDDELL J.E. – Histology of the humann eye. Saunders, Philadelphia PA 1971
(34) HOH S.T., GREENFIELD D.S., LIEBMANN J.M., MAW R., ISHIKAWA H., CHEW S.J., RITCH R. – Factors affecting image acquisition during scanning laser polarimetry. Ophthalmic Surg Lasers 1998; 30: 545-551
(35) HOYT W.H., FRISEN L., NEWMAN N.M. – Fundoscopy of nerve fiber layer defects in glaucoma. Invest Ophthalmol 1973; 12: 814-829
(36) HUANG D., SWANSON E.A., LIN C.P., SCHUMAN J.S., STINSON W.G., CHANG W., HEE M.R., FLOTTE T., GREGORY K., PULIAFITO C.A., FUJIMOTO J.G. – Optical coherence tomography. Science 1991; 254: 1178-1181
(37) HUANG X.R., KNIGHTON R.W. – Linear birefringence of the retinal nerve fiber layer measured in vitro with a multispectral imaging micropolarimeter. J Biomed Opt 2002; 7: 199-204
(38) HUANG X.R., KNIGHTON R.W. – A theoretical model of the polarization properties of the retinal nerve fiber layer in reflection. Appl Opt 2003; 42: 5726-5736
(39) HUANG X.R., KNIGHTON R.W. – Diattenuation and polarization preservation of retinal nerve fiber layer. Appl Opt 2003; 42: 5737-5743
(40) HUANG X.R., KNIGHTON R.W., BAGGA H., VESSANI R., LIEBMANN J.M., RITCH R. – Birefringence of retinal nerve fiber layer in normal human subjects. Invest Ophthalmol Vis Sci 2003; 44 (ARVO e-abstract): 3363
(41) HUANG X.R., BAGGA H., GREENFIELD D.S., KNIGHTON R.W. – Variation of Peripapillary Retinal Nerve Fiber Layer Birefringence in Normal Human Subjects. Invest Ophthalmol Vis Sci 2004; 45: 3073-3080
(42) HUANG X.-R., KNIGHTON R.W. – Microtubules contribute to the birefringence of retinal nerve fiber layer. Invest Ophthalmol Vis Sci 2005, In press
(43) HUANG Y.J., CIDECIYAN A.V., PAPASTERGIOU G.I., BANIN E., SEMPLE-ROWLAND S.L., MILAM A.H., JACOBSON S.G. – Relation of optical coherence tomography to microanatomy in normal and rd chickens. Invest Ophthalmol Vis Sci 1998; 39: 2405-2416
(44) JANKNECHT P., FUNK J. – Optic nerve head analyser and Heidelberg retina tomograph: accuracy and reproducibility of topographic measurements in a model eye and in volunteers. Br J Ophthalmol 1994; 78: 760-768
(45) KLIGER D.S., LEWIS J.W., RANDALL C.E. – Polarized light in optics and spectroscopy. Academic Press Inc, New York NY 1990; 9-18

(46) KNIGHTON R.W., JACOBSON S.G., ROMAN M.I. – Specular reflection from the surface of the retina. Proc SPIE 1989; 1066: 10
(47) KNIGHTON R.W., JACOBSON S.G., KEMP C.M. – The spectral reflectance of the nerve fiber layer of the macaque retina. Invest Ophthalmol Vis Sci 1989; 30: 2392-2402
(48) KNIGHTON R.W., BAVEREZ C., BHATTACHARYA A. – The directional reflectance of the retinal nerve fiber layer of the toad. Invest Ophthalmol Vis Sci 1992; 33: 2603-2611
(49) KNIGHTON R.W. – Quantitative reflectectometry of the ocular fundus. IEEE engineering in medical & biology 1995; 26: 1492-1499
(50) KNIGHTON R.W., ZHOU Q. – The relation between reflectance and thickness of the retinal nerve fiber layer. J Glaucoma 1995; 4: 117-123
(51) KNIGHTON R.W., HUANG X.R., ZHOU Q. – Microtubule contribution to the reflectance of the retinal nerve fiber layer. Invest Ophthalmol Vis Sci 1998; 39: 189-193
(52) KNIGHTON R.W., HUANG X.R. – Directional and spectral reflectance of the rat retinal nerve fiber layer. Invest Ophthalmol Vis Sci 1999; 40: 639-647
(53) KNIGHTON R.W., HUANG X.R. – Visible and near-infrared imaging of the nerve fiber layer of the isolated rat retina. J Glaucoma 1999; 8: 31-37
(54) KNIGHTON R.W., QIAN C. – An optical model of the human retinal nerve fiber layer: implications of directional reflectance for variability of clinical measurements. J Glaucoma 2000; 9: 56-62
(55) KNIGHTON R.W., HUANG X.R. – Linear birefringence of the central human cornea. Invest Ophthalmol Vis Sci 2002; 43: 82-86
(56) KNIGHTON R.W., HUANG X.R. – Analytical methods for scanning laser polarimetry. Opt Exp 2002; 20: 1179-1189
(57) MAKSIMOVA I.L., IZOTOVA V.F., ROMANOV S.V. – Influence of the multiple scattering on the polarization characteristic of bio objects. SPIE 1997; 2981: 220-229
(58) MCCALLY R.L., FARRELL R.A. – Light scattering from cornea and corneal transparency. In: Master B.R. (ed.) Noninvasive diagnostic techniques in ophthalmology. Springer-Verlag, New York NY 1990; 180-210
(59) OGDEN T.E. – Nerve fiber layer of the primate retina: thickness and glial content. Vision Res 1983; 23: 581-587
(60) OGDEN T.E. – Nerve fiber layer of the primate retina: morphometric analysis. Invest Ophthalmol Vis Sci 1984; 25: 19-29
(61) OLDENBOURG R., SALMON E.D., TRAN P.T. – Birefringence of single and bundled microtubules. Biophysical Journal 1998; 74: 645-654
(62) POLLOCK S.C., MILLER N.R. – The retinal nerve fiber layer. Int Ophthalmol Clin 1986; 26: 201-221
(63) QUIGLEY H., MILLER N.R., GEORGE T. – Clinical evaluation of nerve fiber layer atrophy as an indicator of glaucomatous optic nerve damage. Arch Ophthalmol 1980; 98: 1564-1571
(64) QUIGLEY H.A., KATZ J., DERICK R.J., GILBERT D., SOMMER A. – An evaluation of optic disc and nerve fiber layer examinations in monitoring progression of early glaucoma damage. Ophthalmol 1992; 99: 19-28
(65) SATO H., ELLIS G.W., INOUE S. – Microtubular origin of mitotic spindle form birefringence. J Cell Biol 1975; 67: 501-517
(66) SCHUMAN J.S., HEE M.R., PULIAFITO C.A., WONG C., PEDUT-KLOIZMAN T., LIN C.P., HERTZMARK E., IZATT J.A., SWANSON E.A., FUJIMOTO J.G. – Quantification of nerve fiber layer thickness in normal and glaucomatous eyes using optical coherence tomography. Arch Ophthalmol 1995; 113: 586-596
(67) SHURCLIFF W.A. – Polarized light. Harvard University Press, Cambridge MA 1962; 1-14, 68-74
(68) SNELL F. – Physical principles of biological membranes. Gordon and Breach Science Publishers, New York NY 1970; 18-21
(69) SNYDER A.W., MENZEL R. – Photoreceptor Optics. Springer-Verlag, New York NY 1975; 1-13
(70) SOMMER A., KATZ J., QUIGLEY H., MILLER N.R., ROBIN A.L., RICHTER R.C., WITT K.A. – Clinically detectable nerve fiber atrophy precedes the onset of glaucomatous field loss. Arch Ophthalmol 1991; 109: 77-83
(71) VAN BLOKLAND G.J. – Ellipsometry of the human retina in vivo: preservation of polarization. J Opt Soc Am 1985; 2: 72-75
(72) VAN BLOKLAND G., VERHELST S.C. – Corneal polarization in the living human eye explained with a biaxial model. J Opt Soc Am 1987; 4: 82-90
(73) VAN DE HULST H.C. – Light scattering by small particles. Dover, New York NY 1957; 297-326

(74) VAN NORREN D., TIEMEIJER L.F. – Spectral reflectance of the human eye. Vision Research 1986; 26: 313-320
(75) VARMA R., SKAF M., BARRON E. – Retinal nerve fiber layer thickness in normal human eyes. Ophthalmol 1996; 103: 2114-2119
(76) WEALE R.A. – Sex, age and the birefringence of the human crystalline lens. Exp Eye Res 1979; 29: 449-461
(77) WEBB R.H., HUGHES G.W., DELORI F.C. – Confocal scanning laser ophthalmoscope. Appl Opt 1987; 26: 1492-1499
(78) WEINREB R.N., DREHER A.W., COLEMAN A., QUIGLEY H., SHAW B., REITER K. – Histopathologic validation of Fourier-ellipsometry measurements of retinal nerve fiber layer thickness. Arch Ophthalmol 1990; 108: 557-560
(79) WEINREB R.N., BOWD C., GREENFIELD D.S., ZANGWILL L.M. – Measurement of the magnitude and axis of corneal polarization with scanning laser polarimetry. Arch Ophthalmol 2002; 120: 901-906
(80) WHEATER P.R., BURKITT H.G., DANIELS V.G. – Functional histology. Longman Group, London 1987; 321-323
(81) ZHOU Q., KNIGHTON R.W. – Light scattering and form birefringence of parallel cylindrical arrays that represent cellular organelles of the retinal nerve fiber layer. Appl Opt 1997; 36: 2273-2285
(82) ZHOU Q. – System and method for determining birefringence of anterior segment of a patient's eye. Laser Diagnostics Technologies Inc, San Diego CA 2002
(83) ZHOU Q., WEINREB R.N. – Individualized compensation of anterior segment birefringence during scanning laser polarimetry. Invest Ophthalmol Vis Sci 2002; 43: 2221-2228

.....

Corresponding address:

Xiangrun Huang, PhD
Bascom Palmer Eye Institute
University of Miami School of Medicine
1638 N.W., 10th Ave., Miami FL 33136
++ 1-305-326 6000 ext. 4242
Xhuang3@med.miami.edu